HYDROLOGICAL PROCESSES
Hydrol. Process. **26**, 3003–3011 (2012)
Published online 16 December 2011 in Wiley Online Library
(wileyonlinelibrary.com) DOI: 10.1002/hyp.8289

Screening the current soil drainage class map of Flanders (Belgium) for its predictive quality

J. Van de Wauw* and P. A. Finke

Department of Geology and Soil Science, Universiteit Gent, Krijgslaan 281/S8, B-9000 Gent, Belgium

Abstract:

The predictive quality of the current drainage class map of Flanders was evaluated using data from two monitoring networks: one with good spatial coverage but poor temporal coverage and another with better temporal but poor spatial coverage. We combine both networks to obtain 1678 point predictions for mean highest water (MHW) and mean lowest water (MLW) tables by applying time series modelling and total least squares regression. The resulting MHW and MLW point data set was used to evaluate the currency of the existing map and to identify regional differences. The quality of the current map is moderate, and large differences occur between regions. Especially the Campine region shows large and systematic differences, whereas the southeastern hills and chalk–loam region is relatively accurate. If more weight is given to errors in the wetter drainage classes, about 50% of the area of Flanders would benefit from remapping. Copyright © 2011 John Wiley & Sons, Ltd.

KEY WORDS water table; map; accuracy; phreatic groundwater; map purity; time series model; impulse-response function

Received 28 January 2011; Accepted 13 July 2011

INTRODUCTION

Because of its shallow depth, phreatic groundwater dynamics are one of the most important land characteristics for agriculture, nature development and other land uses. In Flanders, these dynamics are usually estimated from the natural drainage classes that are indicated on the Belgian soil map (1/20.000), based on data collected during the national soil survey (1947–1971). The natural drainage condition depicted on the soil maps was derived from the depth of gley mottles and the reduction horizon and the position in the landscape. It is indicated using combined classes of the depth of the reduction horizon and the depth of gley mottles, and the unified legend is given in Figure 1 (Van Ranst and Sys, 2000). Originally some map sheets used a slightly different definition. For example De Coninck (1957) and Snacken (1964) defined the drainage classes only based on the depth of mottling and the duration that the water level would exceed a threshold. The fact that different map sheets used different definitions while mapping implies that some error is made when applying the unified legend everywhere. The coastal region (6% of the area) was mapped using a geomorphological–lithostratigraphical legend, which does not include a drainage class. Because a conversion table (Sevenant *et al*., 2002) is frequently used to derive a drainage class, this table was applied and the resulting drainage class map was joined with the other (94% of the area) map.

*Correspondence to: J. Van de Wauw, Department of Geology and Soil Science, Universiteit Gent, Krijgslaan 281/S8, B-9000 Gent, Belgium. E-mail: Johan.vandewauw@gmail.com

Although the original definition was morphological, a common interpretation (eg. Vandamme and De Leenheer, 1969, Boucneau *et al*., 1996) of these drainage classes is a combination of intervals for mean highest and mean lowest groundwater levels. The mean highest water level (MHW) and mean lowest water level (MLW) are defined, respectively, as the mean value of the three highest and lowest groundwater levels measured biweekly or semi-monthly for at least 8 years, preferably longer (30 years) for climate representativeness (Van der Sluijs and De Gruijter, 1985).

Although all studies agree that there is a strong relationship between these morphological features and the water table, both overestimations and underestimations are reported when the depth of mottling is converted to the MHW. One study was done between 1963 and 1968 in the Campine region by Vandamme and De Leenheer (1969). Based on their observations in 54 piezometers on sandy and sandy–loamy soils, they proposed the levels for MHW/MLW in sandy soils in Table I, which are in fact slightly "wetter" than would be expected from directly using the depth of gley mottles.

Also, studies in other regions show that both overestimations can occur when the depth of mottling is used to estimate the depth of the water table. Van Wallenburg (1973) made a distinction between brown mottles and grey mottles. Brown mottles in alluvial soils often occur above the MHW, whereas the upper boundary of grey mottles seems to occur at about 30 cm below the MHW. The relation between the reduction horizon and the MLW was good. Also, Genthner *et al*. (1998) reported underestimation of high water levels and attributed this to the lack of easily oxidisable organic carbon. Overestimations have also been reported (Jacobs *et al*., 2002), but in relict

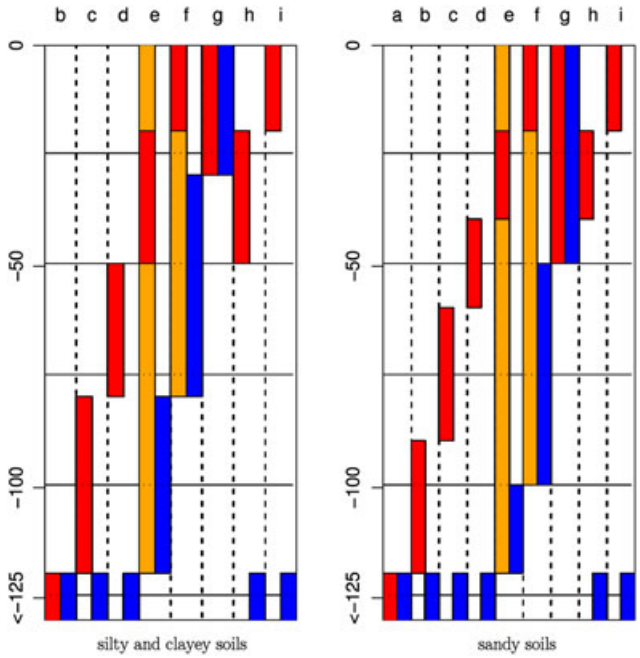

Figure 1. Drainage class (a–i) definitions according to Van Ranst and Sys (2000) as depth intervals (cm). The dark grey areas indicate the upper limit of mottling and are interpreted as MHW; the black areas indicate the upper limit of reduction and are interpreted as MLW. The definition for the upper boundary of mottling was expanded in classes e and f (light grey areas) to handle combinations of mottling/reduction which were previously not defined

Table I. Proposed MHW and MLW levels for sandy soils in the Campine region ((Vandamme and De Leenheer, 1969), Table 12)

	Drainage class				
	a	b	c	d	e
MHW	>120	80–120	50–80	20–50	<20
MLW	>240	180–240	150–180	120–150	80–120

landscape features in regions which are not comparable with the Belgian situation.

Nevertheless, the common interpretations use the same depth for MHW/MLW and gley mottles/reduction horizon, respectively. To screen the currency of this interpretation of the soil drainage class map, the mapped units are compared with recent point estimates of MHW/MLW. Such estimates can be obtained from phreatic groundwater monitoring networks. One such a network has a good spatial coverage (average density of 1/680 ha) but a poor temporal coverage because the monitoring started only in 2004–2006 and only two observations are made per year. Existing but smaller networks (referred to as reference time series from this point) have a better temporal coverage but only a poor spatial coverage. This means that it is beneficial to combine both types of network to derive MHW/MLW statistics. This comparison can be made for different regions and different drainage classes to identify regions where map quality is insufficient.

METHODOLOGY

Reference time series

Two monitoring networks are used as a reference time series for calculating the groundwater statistics: the phreatic filters of the primary network of the Flemish Environmental Agency (VMM) and the monitoring networks installed in nature reserves. An initial selection was made: all locations with at least 2 years of measurements and 24 observations were included. A visual screening was done to exclude series with trends indicating strong recent human impacts such as changed groundwater extraction, wetland restoration projects, etc. After time series modelling (next section), a further selection was done to remove time series without a sufficiently good model fit (explained variance percentage <60%) and/or time series which were too short to validate the predicted interyearly variation.

Time series modelling

The monitoring period in some reference series was too short for the direct calculation of MHW and MLW, which requires at least 8 years of measurements. Moreover, the monitoring periods have different lengths and may not cover the same periods. This can lead to biased estimations because precipitation surplus is a major driving factor in groundwater fluctuations in western European climate (Knotters and Bierkens, 2000), and precipitation surplus varies by year. Therefore, a time series model was fitted to the phreatic groundwater level, which combines precipitation and potential evapotranspiration to precipitation surplus as a driver variable to estimate water table depth. The time series model used is PIRFICT (von Asmuth *et al.*, 2002). This time series model was chosen because it supports fitting time series models to irregular time series and because it proved to perform well in various situations (von Asmuth *et al.*, 2002).

The PIRFICT model is an impulse-response model that consists of three parts: a base drainage level (d), a deterministic part $h^{\mathrm{det}}(t)$ and a stochastic part $n(t)$ (all in meters).

$$h(t) = h^{\mathrm{det}}(t) + n(t) + \mu$$
$$h^{\mathrm{det}}(t) = \int_{-\infty}^{t} \frac{Aa^n t^{n-1} e^{-a(t-\tau)}}{\Gamma(n)} p(\tau) d\tau \quad (1)$$
$$n(t) = \int_{-\infty}^{t} \sqrt{2\alpha\sigma_n^2} e^{-\alpha(t-\tau)} dW\tau$$

with

- $h(t)$ as the observed groundwater level (m) at time t (days)
- precipitation surplus (m)
- the deterministic component of the groundwater level attributable to the precipitation surplus $p(t)$ (m)
- the residual series, a continuous stochastic process, where $W(t)$ is a continuous white noise (Wiener) process with $E(W[t]) = 0E[\mathrm{d}W(t)2] = \mathrm{d}tE[W(t1), W(t2)] = 0$
- the variance of the residuals of the deterministic model (m^2).

The three parameters of the deterministic model (A, a, n) and the parameter α of the stochastic model are estimated during the calibration phase, as is the ratio between precipitation and evapotranspiration. After calibration, 100 stochastic simulations over a fixed time frame of 30 years (1978–2008) were done to derive MHW and MLW. In addition, these simulations provided interpolated water levels for days without measurements, which are needed when the data of these reference series are combined with the measurements of the phreatic groundwater monitoring network (cf. next section).

Short time series

The phreatic groundwater monitoring network (Figure 2), implemented and managed by the Flemish Environmental Agency (VMM), was built as a consequence of the European Nitrate Directive (91/676/EEG). The network contains 2071 monitoring sites, equivalent to a density of 1/680 ha. These points are measured two times per year, generally in spring and autumn. Monitoring piezometers cover Flanders more or less equally but have a higher density in regions more vulnerable to nitrate leaching (Eppinger and Thomas, 2007). A selection of 1545 piezometers of this network was made with shallow filters (less than 5 m) because drainage classes are related to phreatic water table measurements. In addition, all time series from the reference networks which could not be modelled were added to the selection of short time series.

Stratification

Prior to combining the short time series with the reference time series, the region of Flanders was divided in strata according to the map of ecoregions (Figure 3; Sevenant *et al.* (2002)), which groups regions with similar properties concerning geology, geomorphology, hydrology and groundwater. It was chosen among other stratification options (maps of agricultural regions, phreatic groundwater bodies and the soil association map) because most of the units of the maps contain enough observations in the different drainage classes while still offering enough detail to distinguish regional differences regarding updating needs and/or trends due to climate, diffuse human influence or different mapping standards. The small ecoregions gravel rivers and chalk region were omitted because no phreatic groundwater records were available for these regions. The southeastern hills and chalk–loam region were combined to contain enough observations in the different drainage classes.

Combining the reference time series and the phreatic network data

To estimate descriptive statistics like MHW and MLW for round water time series containing only a small number of observations, linear regression can be used to create a relationship between observations in the short time series and the reference time series in the same stratum. Because in many cases the reference series were not measured on the same day as the short time series, this method has to be adjusted: it relies on a relationship between the water level measured in the reference series on a specific date and the groundwater statistics derived in these series. If no observation is available, the mean simulated water table on that specific date is used. This introduces uncertainty in the explanatory variable in both methods, which can cause problems with the standard least squares algorithms because they do not take this uncertainty into account. Instead, weighted total least square regression (Markovsky and Van Huffel, 2007) is used, which incorporates (and weighs for) not only the uncertainty in the predicted variable (ε) but also the uncertainty (η) in the explanatory variable.

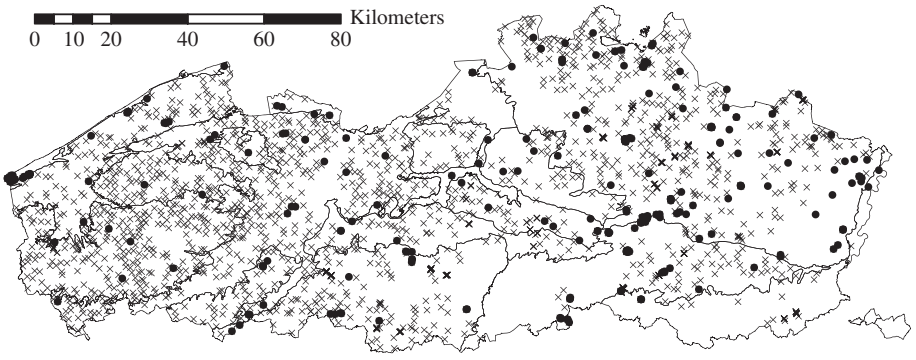

Figure 2. Location of the long reference series (black circles) and the phreatic groundwater monitoring network (gray crosses)

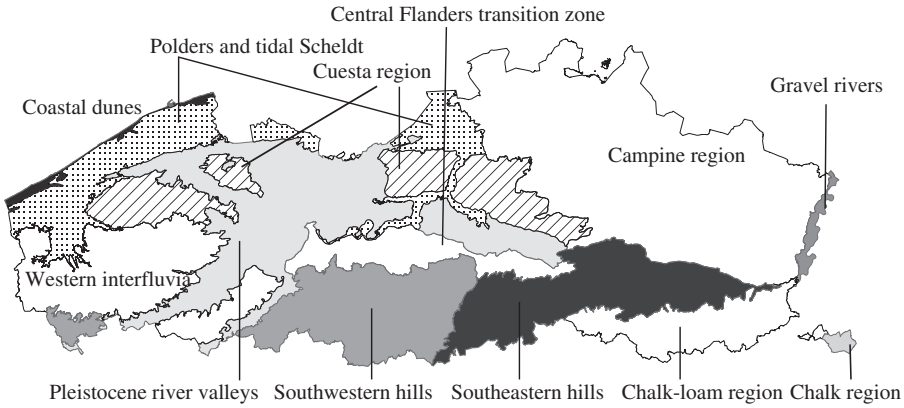

Figure 3. Ecoregions of Flanders. The small gravel rivers and chalk regions were omitted because no phreatic groundwater records were available for those regions. The southeastern hills and chalk–loam regions were combined to contain enough observations in the different drainage classes

$$y = \alpha + (x + \eta)\beta + \varepsilon \tag{2}$$

In comparison with ordinary least squares, this gives more weight to more certain observations and generally leads to a steeper regression curve (Figure 4). To solve the regression, the algorithm by Krystek and Anton (2007) was implemented in R (R Development Core Team, 2011). This method also gives the uncertainty matrix for the regression coefficients (α, β), which makes it possible to calculate the variance of the prediction error for a new x with its corresponding uncertainty (η):

$$\begin{aligned}\mathrm{Var}(\hat{y}) = {} & \mathrm{Var}(\alpha) + \mathrm{Var}(\beta)(x)^2 + \beta^2\mathrm{Var}(\eta) \\ & + \mathrm{Cov}(\alpha, \beta)x + \mathrm{Var}(\varepsilon)\end{aligned} \tag{3}$$

Two methods (Figure 5) have been proposed to link observations in reference piezometers and short time series: the first method (Socolow *et al.*, 1994, Oude Voshaar and Stolp, 1997) can be used when at least four observations are available in the short time series. In this case, linear regression is used to fit a relationship between the observations in the short time series (z_s) and the observations in each of the reference series (z_r) for every date with a measurement in the short time series.

$$\forall i \in (\text{reference series}) : z_{s,t} = \alpha_i z_{i,t} + \beta_i + \varepsilon_i \tag{4}$$

The best relationship (i.e. with the best fitting reference series) is then retained and used for predicting the MHW of the short series ($\mathrm{MHW_s}$) as a function of the MHW in the reference series ($\mathrm{MHW_r}$):

$$\mathrm{MHW_s} = \alpha_i \mathrm{MHW_r} + \beta_i \tag{5}$$

The second method (te Riele and Brus, 1991, Finke *et al.*, 2004) was developed for estimating the MHW and MLW table using only two well-timed observations in the short time series, in winter and summer, when the groundwater table is close to the MHW and MLW, respectively. This method consists of two steps:

1. For every day with a measurement in the short time series, a linear relationship between the observations in all the reference time series and the MHW in those series:

$$\begin{aligned}\forall t \in (\text{dates in short time series}) : z_s \\ = \alpha_t z_{r,t} + \beta_t + \varepsilon_t\end{aligned} \tag{6}$$

2. These relationships are applied for every day in the short time series; the model on the date d with the lowest prediction error is retained:

$$\mathrm{MHW_s} = \alpha_t z_{t,r} + \beta_t \tag{7}$$

Both methods are applied to all short time series, and the MHW/MLW predictions with the lowest prediction errors (Eq. 3) were selected for further analysis, but only if the standard error of the prediction was less than 20 cm.

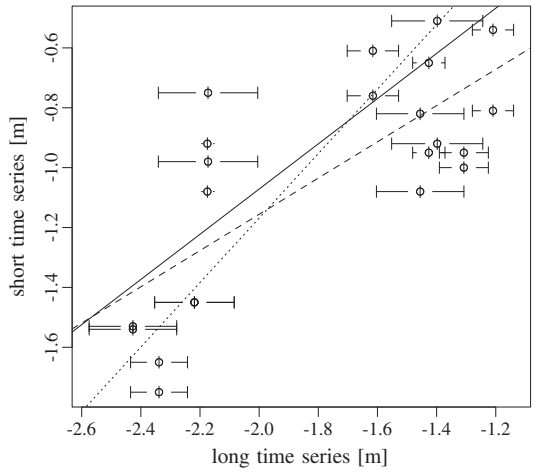

Figure 4. Comparison of weighted least squares regression of $\boldsymbol{y = f(x)}$ (dashed line), the weighted least square regression of $\boldsymbol{x = f(y)}$ and weighted total least squares regression (solid line). The angle of the total least squares regression is between these two regression lines and therefore steeper than the ordinary or weighted least square regression

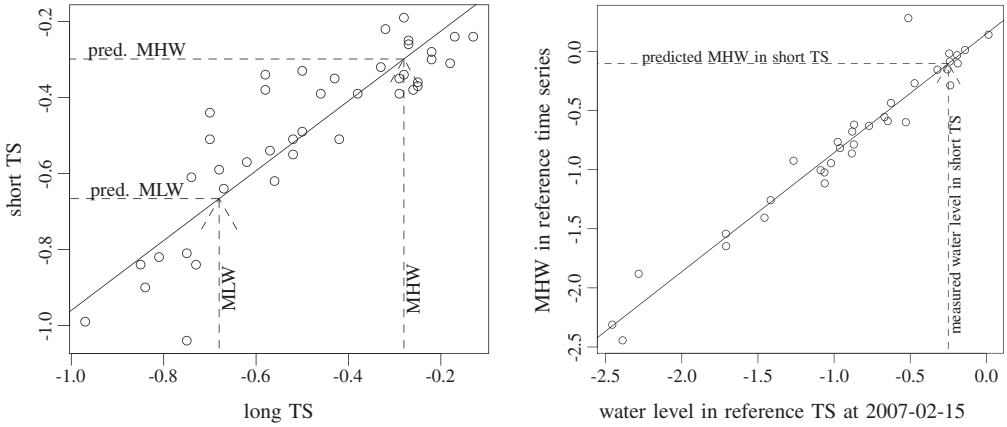

Figure 5. Comparison of two methods to predict MHW/MLW in short time series based on the measurements (meters) in the reference time series: the first method (left graph) uses all observations of the short time series and fits a relationship with one reference time series. The second method (right graph) uses a relationship between the water level and the MHW/MLW in all reference series within a stratum on a specific date

QUALITY CRITERIA

Map purity and error matrix

One way to evaluate the quality of the map is by looking to the map purity: the fraction of the area in which depicted classes are correct. A contingency table or error matrix is made for every ecoregion with the calculated drainage class and the original map. To calculate the purity, in each test location an indicator IE is calculated, which takes the value 0 if the drainage class on the map does not match the calculated drainage class and 1 else (if the original map contains complexes of drainage classes, a value of 1 is attributed for all possibilities of the complex). The classic approach to calculate the map purity for a combination of drainage class (dc) and region (r) is using the average value of these indicators:

$$\hat{p}_{\mathrm{dc,r}} = c/(c+n) \tag{8}$$

with

- c as the number of correct predictions (−)
- n as the number of non-correct predictions (−)

There are two problems with this approach: it does not take into account the uncertainty of the estimated drainage class (which will be covered in the next section), and it does not allow the calculation of a reliable confidence interval of the purity, even with large sample sizes (see, e.g. Brown *et al.* (2001)). Although more elaborate techniques exist (Brown *et al.*, 2002), a simple way to calculate a more reliable confidence interval for a 95% probability is to add four pseudo-observations (Wilson, 1927, Agresti and Coull, 1998): two successes and two failures. The estimated mean indicator value or expected map purity then becomes

$$\begin{aligned}\mathrm{MIE}_{\mathrm{dc,r}} &= E\left(\mathrm{IE}_{\mathrm{dc,r}}\right) = \tilde{p}_{\mathrm{dc,region}} \\ &= (c+2)/(c+n+4)\end{aligned} \tag{9}$$

and its corresponding variance (Agresti and Coull, 1998) is

$$\mathrm{Var}(\mathrm{MIE_r}) = \sqrt{\tilde{p}(1-\tilde{p})/(n+4)} \tag{10}$$

For the aggregate data per region, the map purity for a whole region is calculated as a weighted average, using the relative area ($a_{\mathrm{dc,r}}$) as weight factor.

$$a_{\mathrm{dc,r}} = A_{\mathrm{dc,r}} / \sum_{\mathrm{dc}=a}^{i} A_{\mathrm{dc,r}} \tag{11}$$

$$\mathrm{MIE_r} = \sum_{\mathrm{dc}=a}^{i} \mathrm{MIE}_{\mathrm{dc,r}} \times a_{\mathrm{dc,r}} \tag{12}$$

The variance of this weighted average can be calculated accordingly (de Gruijter *et al.*, 2006):

$$\mathrm{Var}\left(\mathrm{MIE}_{\mathrm{region}}\right) = \sum_{\mathrm{dc}=a}^{i} a_{\mathrm{dc,region}}^2 \mathrm{Var}\left(\mathrm{MIE}_{\mathrm{dc,region}}\right) \tag{13}$$

This approach assumes that the piezometers are spatially independent. Experimental variograms of $\mathrm{IE_{r,dc}}$ were constructed in strata with more than 20 observations to validate this assumption. Although some spatial correlation could be observed in four combinations of drainage class and regions (Figure 6), it was not observed in eight other combinations. Moreover, the usage of declustering weights (using voronoi polygons) only had a very small effect on MIE ($< 0.5\%$) in these cases, and they were therefore not included in the rest of the analysis.

Following a similar approach, it is possible to evaluate in which locations the drainage class is only one class off (MIE1).

Fuzzy map purity

Instead of using a binary indicator IE when calculating the map purity, the probability that an observation falls within a drainage class can be used. This probability can be calculated by using the bivariate (MHW and MLW)

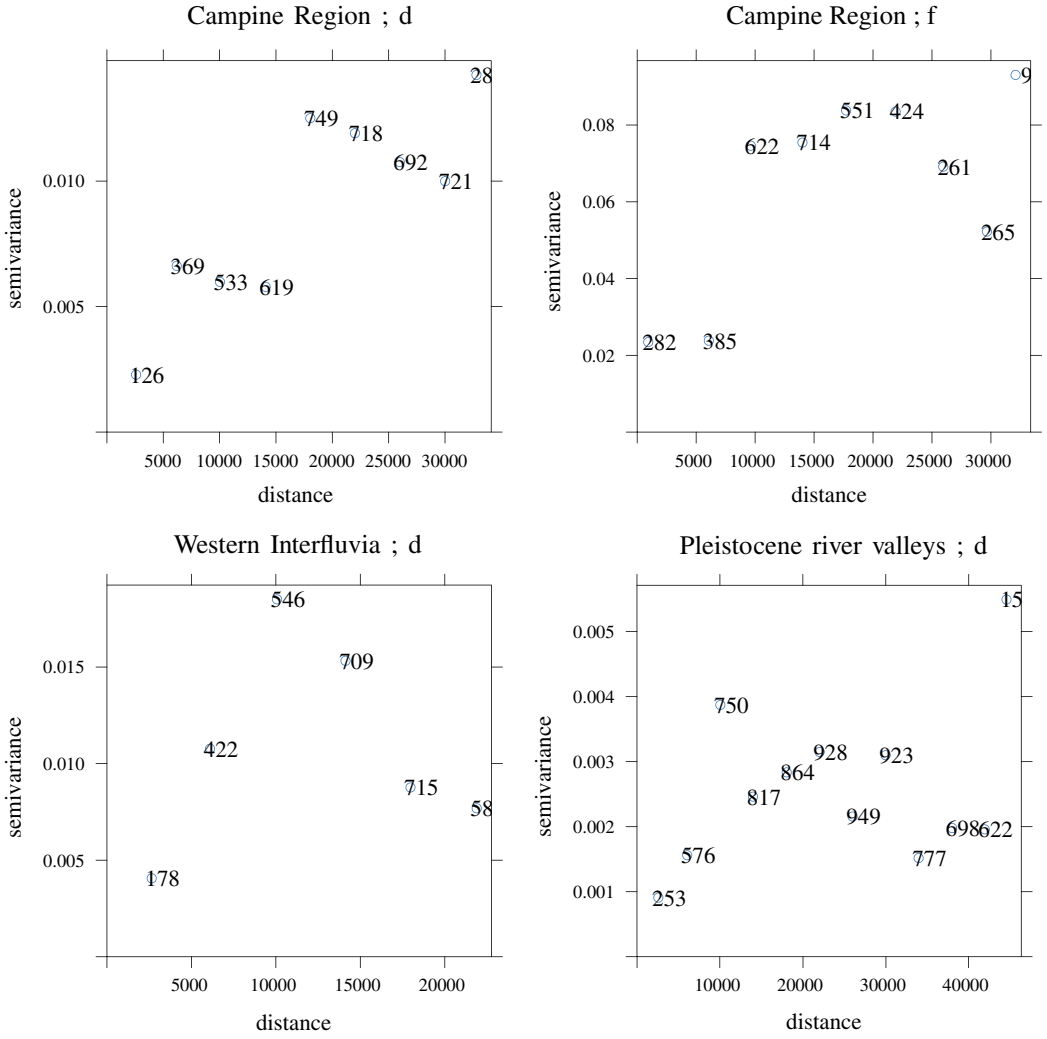

Figure 6. Selected robust variograms (Cressie, 1993, Pebesma, 2004) of $\mathbf{IE_{dc,r}}$ for combinations of region and drainage classes where spatial autocorrelation is present

density distribution (Figure 7). The effect is that the error matrix will not contain hard indicator values but the probabilities for class membership. Errors in MHW and MLW are assumed to be uncorrelated. A small proportion of the distribution is not assigned to a drainage class (extragrades, X in Figure 7), because MLW is higher than MHW, which is impossible due to their definitions. This proportion was always very small and therefore omitted.

Mean (absolute) error

A second quality criterion is based on the distance of the MHW and MLW (for short, MxW) to the nearest class boundaries in centimetres. This value (E_{MxW}) is defined as the number of centimetres that the actual value of MxW is outside the class boundaries, expressed in centimetres from the surface. A positive value of E_{MxW} therefore indicates a drier situation than previously mapped.

$$E_{MxW}(dc, MxW_v) = \begin{cases} MxW_v < MxW_{dc,min} < MxW_v < MxW_{dc,max} & : 0 \\ MxW_v < MxW_{dc,min} & : MxW_{dc,min}\text{-}MxW_v \\ MxW_v > MxW_{dc,max} & : MxW_v\text{-}MxW_{dc,max} \end{cases} \quad (14)$$

with

- MxW_v as the value of MxW in the validation set
- $MxW_{dc,min}MxW_{dc,min}$ as the lower boundary of MxW specified for the mapped drainage class.

The mean absolute E (MAE) and mean E (ME) are defined as the average deviation of all MxW predictions within a stratum from the nearest boundary, weighted by the area of the corresponding drainage classes.

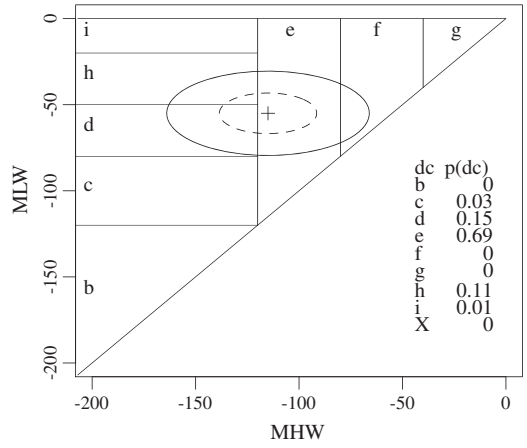

Figure 7. Illustration of the calculation of the fuzzy MIE. Instead of assigning a value of 1 to the drainage class e and 0 to the other classes, the uncertainty of the estimate sdMHW = 20 cm, sdMLW = 10 cm, illustrated by ellipses (50% and 95% confidence level), is used

$$\mathrm{MAE}_{\mathrm{MxW}} = \sum_{i=1}^{n} a_{\mathrm{dc}} |\mathrm{E}_{\mathrm{MxW}}(i)| (\mathrm{cm}) \tag{15}$$

$$\mathrm{ME}_{\mathrm{MxW}} = \sum_{i=1}^{n} a_{\mathrm{dc}} \mathrm{E}_{\mathrm{MxW}}(i) (\mathrm{cm}) \tag{16}$$

RESULTS AND DISCUSSION

Calculation of MxW in reference time series

From the total number of 384 reference series, 247 reference time series (Figure 2) could be retained, 58 of which had an observation time span of less than 5 years.

Quality of MxW point estimates

Figure 8 shows the distribution of the standard error of the prediction of MHW and MLW. On average, the standard prediction error was 12.3 cm for MHW and 13.3 cm for MLW. From the original 1930 locations (1545 from the phreatic groundwater monitoring network, 138 short and 247 reference time series from other networks), 1678 could be retained which have standard errors for MHW and MLW lower than 20 cm.

Map purity

The differences between the fuzzy map purity and the map purity are small. This indicates that classification errors due to the uncertainty in the MHW/MLW estimates seem to level each other out in the majority of the regions. Nevertheless, a comparison using both the corrected and uncorrected map purity shows that this correction matters when only a small number of observations is present in one stratum. The difference is most evident in the southeastern hills and chalk–loam region, where a large part of the area is covered by one drainage class with few observations. The indicator of error including one class off (MIE1) would equal $93.3\% \pm 1.4\%$ when using Equation (8) *versus* $71.7\% \pm 13.8\%$ when using Equation (9). In other regions, the differences in MIE are smaller than 5%, and the differences in sd(MIE) are smaller than 0.5%. Also, the differences between MIE and fuzzy MIE (Table II) are small.

Quality of existing drainage class maps

Table II shows the quality parameters of the drainage map for the different ecoregions. The map purity was largest in the combined southeastern hills and chalk–loam region. This also results in low values for MAE and ME. These results can be attributed to a large share of the map with a dry drainage class (b) which remained dry. It is, however, based on relatively few observations, which leads to the high standard error for the map purity in this region. The other regions show a map purity ($\mathrm{MIE}_{\mathrm{r}}$) below 30%, and most regions have more than 50% of the area more than one drainage class off ($\mathrm{MIE1}_{\mathrm{r}}$). Overall, we can observe that using the statistical estimations of MHW and MLW only 25.5% of the area corresponds to the true drainage class, but the

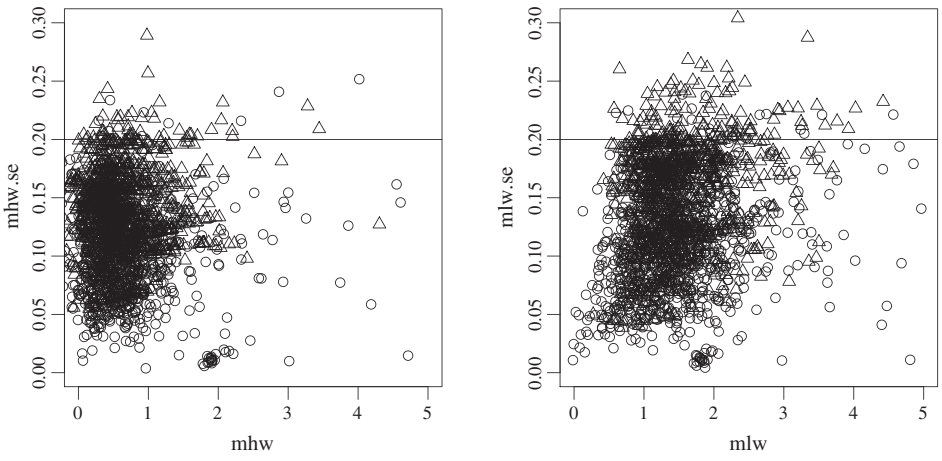

Figure 8. Predicted MHW and MLW (in meters) with their standard errors. Circles are the result of regression with one long time series, and triangles are the result of a regression with all time series in a stratum at a set date. Only predictions with a standard error of less than 0.2 m were retained for the rest of the analysis

Table II. Quality parameters of the drainage class maps per region. The quality parameters are explained in formula 9-16.

Region	No. of locations	Surface (ha)	MIE ±sd(MIE) (%)	MIE1 sd(MIE) (%)	Fuzzy MIE sd (%)	FuzzyMIE1 ±sd (%)	MAE_{MHW} (cm)	MAE_{MLW} (cm)	ME_{MHW} (cm)	ME_{MLW}
Southeastern hills and chalk–loam region	91	59014	57.6 ± 15.4	71.7 ± 13.8	59.1 ± 15.2	71.2 ± 13.8	7.4	2.8	3.2	−0.8
Polders and tidal Scheldt river	123	89829	29.9 ± 4.1	61.2 ± 4.4	22.2 ± 3.7	49.3 ± 4.5	15.9	14.8	10.4	6.5
Cuesta region	148	95268	24.1 ± 3.3	49.3 ± 3.9	23.4 ± 3.3	47.0 ± 3.9	17.7	12.4	−6.7	−3.5
Western interfluvia	259	128043	23.4 ± 2.5	49.2 ± 2.8	20.9 ± 2.4	47.2 ± 2.9	22.7	9.3	−3.7	−4.2
Pleistocene river valleys	346	177357	19.9 ± 2.1	48.4 ± 2.6	19.2 ± 2.1	47.8 ± 2.6	20.2	11.3	−8	−2.1
Campine region	466	295389	23.5 ± 2.2	59.1 ± 2.5	21.3 ± 2.1	57.2 ± 2.5	33.6	12.0	28.2	8.8
Central Flanders transition zone	53	45880	26.3 ± 5.7	41.4 ± 6.2	23.4 ± 5.5	42.1 ± 6.3	24.6	15.6	−14.8	−12
Coastal Dunes	29	4559	22.2 ± 6.9	38.8 ± 8.3	21.1 ± 6.8	39.6 ± 8.4	39	3.6	−13	−3.6
Southwestern hills	163	111032	20.3 ± 4.0	36.6 ± 4.5	21.7 ± 4.2	37.6 ± 4.6	36.8	14.6	−31.5	−9.1
Flanders	1678	1005485	25.5 ± 3.6	52.6 ± 3.9	23.4 ± 4.1	47.0 ± 4.4	25.2	11.7	2.7	0.3

error is not larger than one drainage class in half of the area (52.6% in Table II). Overall, there seems to a slightly wetter situation than depicted on the drainage class map, although the ecoregions of the Polders and tidal Scheldt and Campine region show a drier situation.

It remains unclear whether these changes can be attributed to a trend in groundwater levels, rather than due to a systematic error while converting the redoximorphic features to MHW and MLW, combined with possible regional bias because slightly different definitions were originally used when the soil map was made.

Conclusions about the area to be updated in Flanders

Results of map update trials (Finke, 2000, Finke *et al*., 2004, Van de Wauw and Finke, 2008, Finke *et al*., 2010) show that MIE_r ranges between 36% and 65%, MAE_{MHW} between 1 and 6 cm, and MAE_{MLW} up to 14 cm. Based on these results, it seems that the quality of the map for the combined southeastern hills and chalk–loam region can hardly be improved using that methodology, but the rest of Flanders can be improved. A different approach is to decide for every region per drainage class separately whether updating is necessary. This also makes it possible to put emphasis on errors in wetter drainage classes, because an error in those classes is usually more important than that for deeper water tables. One such scenario is described in Table III, and the result is presented in Figure 9. In this scenario, approximately 50% of the mapped area should be remapped.

GENERAL CONCLUSIONS

We have presented a methodology to validate the common interpretation of the drainage class map as a combination of MHW and MLW by using 1684 accurate MHW and MLW estimations. We conclude that the quality of the current drainage class map of Flanders is moderate, and large differences occur between regions. Especially the Campine region shows large error (MAE) and systematic difference (ME), indicating that the situation is drier than depicted on the map. The estimates for the southeastern hills and chalk–loam region seem quite accurate, but the large confidence interval on the map purity proves that this conclusion is only drawn on a small data set. If more weight is given to errors in the wetter drainage classes, about 50% of the area of Flanders would benefit from remapping.

Table III. Critical quality label for $\mathbf{MAE_{MxW}}$ per drainage class in one updating scenario, used in Figure 9.

	Tolerance (cm)	
Drainage class	MAE_{MHW}	MAE_{MLW}
Very wet (f, g)	20	20
Wet (e, h, i)	20	40
Dry (a, b, c, d)	40	40

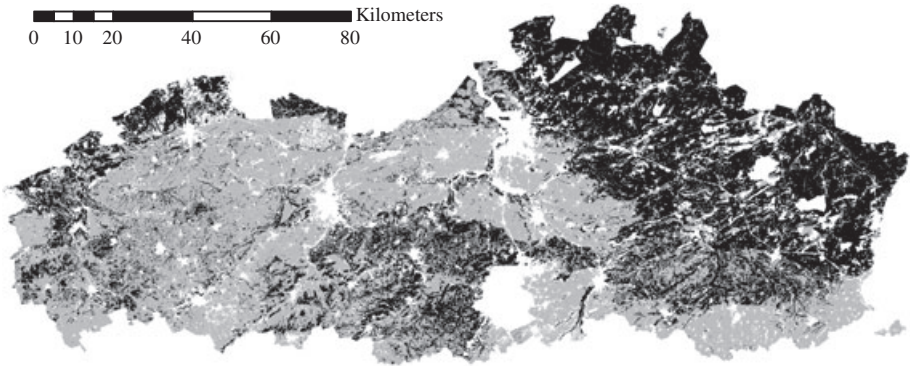

Figure 9. Map updating scenario when the thresholds of Table III are used. The light zones have sufficient quality; in the dark zones, remapping is recommended

ACKNOWLEDGEMENTS

This research was conducted as part of the research project BOD/STUD/2008/03 funded by the Environment, Nature and Energy department (LNE) of the Flemish Government. We also thank Griet Heuvelmans of the Flemish Environment Agency (VMM) for providing the time series of groundwater measurements.

REFERENCES

Agresti A, Coull BA. 1998. Approximate is better than "exact" for interval estimation of binomial proportions. *The American Statistician* **52**(2): 119–126.

von Asmuth JR, Bierkens MFP, Maas K. 2002. Transfer function-noise modeling in continuous time using predefined impulse response functions. *Water Resources Research*, **38**(12): 23.1–23.12.

Boucneau G, Van Meirvenne M, Desmet J, Hofman G. 1996. A methodology to evaluate the reliability of the Belgian soil map for predicting the actual water table characteristics. *Geoderma* **69**(3–4): 193–207.

Brown LD, Cai TT, DasGupta A. 2001. Interval estimation for a binomial pro portion. *Statististical Science* **16**(2): 101–133.

Brown LD, Cai TT, DasGupta A. 2002. Confidence intervals for a binomial proportion and asymptotic expansions. *Annals of Statististics* **30**: 160–201.

Cressie NAC. 1993. *Statistics for Spatial Data*. Wiley.

De Coninck F. 1957. Belgian Soil Map: Addendum for Map Sheet Wuustwezel 7W. Centrum voor Bodemkartering, Gent. in Dutch.

Eppinger R, Thomas PJ. 2007. Hydrogeological homogeneous zones to derive the nitrate vulnerability of ground water. *Tijdschrift Water* **28**: 32–37. in Dutch.

Finke PA. 2000. Updating the (1: 50,000) Dutch groundwater table class map by statistical methods: an analysis of quality versus cost. *Geoderma* **97**(3–4): 329–350.

Finke PA, Brus DJ, Bierkens MFP, Hoogland T, Knotters M, de Vries F. 2004. Mapping groundwater dynamics using multiple sources of exhaustive high resolution data. *Geoderma* **123**(1–2): 23–39.

Finke PA, Van de Wauw J, Baert G. 2010. Development and validation of a methodology to update the drainage class map of Flanders. Final report of Project BODSTUD/2008/03. in Dutch.

Genthner MH, Daniels WL, Hodges RL, Thomas PJ. 1998. Redoximorphic features of the seaonal high water table, Upper Coastal Plain, Virginia. In *Quantifying Soil Hydro-morphology*, Rabenhorst ML, Bell JC, McDaniel J (eds). SSSA/ASA Special Publication, Amer. Soc. Agron.

de Gruijter JJ, Brus DJ, Bierkens MFP, Knotters M. 2006. *Sampling for Natural Resource Monitoring*. Springer, Berlin.

Jacobs PM, West LT, Shawn JN. 2002. Redoximorphic features as indicators of seasonal saturation, Lowndes County, Georgia. *Soil Science Society of America Journal* **66**: 315–323.

Knotters M, Bierkens MFP. 2000. Physical basis of time series models for water table depths. *Water Resources Research* **36**(1): 181–188.

Krystek M, Anton M. 2007. A weighted total least-squares algorithm for fitting a straight line. *Measurement Science and Technology*, **18**(11): 3438–3442.

Markovsky I, Van Huffel S. 2007. Overview of total least-squares methods. *Signal Processing* **87**(10): 2283–2302.

Oude Voshaar J, Stolp J. 1997. Estimating MHW and MLW from temporary piezometers with short time series. Technical Document 30, Winand Staring Centre for Integrated Land, Soil and Water Research. in Dutch.

Pebesma EJ. 2004. Multivariable geostatistics in S: the gstat package. *Computers and Geosciences* **30**: 683–691.

R Development Core Team. 2011. R: A Language and Environment for Statistical Computing. R Foundation for Statistical Computing, Vienna, Austria. URL http://www.R-project.org/. ISBN 3-900051-07-0.

te Riele WJM, Brus DJ. 1991. Methods to estimate MHW from phreatic head measurements. Staring Centrum rapport nr 158, Wageningen. in Dutch.

Sevenant M, Menschaert M, Couvreur M *et al*. 2002. Ecodistricts: tools for an area specific Flemish environmental policy: Action 134 of the Flemish Environmental Policy Plan 1997–2001. Ministry of the Flemish Community. AMINAL. in Dutch.

Snacken F. 1964. Belgian Soil Map: Addendum for Map Sheet Sint-Gillis-Waas 27W. Centrum voor Bodemkartering, Gent. in Dutch.

Socolow RS, Frimpter MH, Turtora M, Bell RW. 1994. A technique for estimating groundwater levels at sites in Rhode Island from observation-well data. US Geological Survey water-resources investigations report 94–7138.

Van de Wauw J, Finke PA. 2008. Mapping phreatic groundwater dynamics in the Dijle valley. In *Book of Abstracts*, Blum WEH, Gerzabek MH, Vodrazka M (eds). EUROSOIL 2008, Soil-Society-Environment, page 145. ISBN 978-3-902382-05-4

Van der Sluijs P, De Gruijter JJ. 1985. Water table classes: A method to describe seasonal fluctuation and duration of water tables on Dutch soil maps. *Agricultural Water Management*, **10**(2): 109–125. DOI: 10.1016/0378-3774(85)90001-0

Van Ranst E, Sys C. 2000. Unified legend to the Belgian Soil Map (scale 1:20000). Laboratory of Soil Science. Ghent University.

Vandamme J, De Leenheer L. 1969. Fluctuations of the water table over a period of 5 years (1963–68) in the sandy soils of the Campine in the province of Antwerp (Belgium). *Pédologie* **19**(3): 275–320. in French.

van Wallenburg C. 1973. Hydromorphic Soil Characteristics in Alluvial Soils in Con-nection with Soil Drainage. Trans. of Comm. V and V1 of the ISSS. Verlag Chemie, Weinheim.

Wilson EB. 1927. Probable inference, the law of sucession, and statistical inference. *Journal of the American Statistical Association* **22**: 209–212.

